

## COMPARATIVE STUDIES ON THE CHARACTERISTIC PROPERTIES OF THE GROUND AND CONVENTIONAL $\text{LaCo}_{0.7}\text{Cu}_{0.3}\text{O}_3$ PEROVSKITE

Received 24 April 2008

NGUYEN TIEN THAO<sup>1</sup>, SERGE KALIAGUINE<sup>2</sup>

<sup>1</sup>Faculty of Chemistry, College of Sciences, Vietnam National University, Hanoi

<sup>2</sup>Department of Chemical Engineering, Laval University, Quebec, Canada, G1K 7P4

### ABSTRACT

*The characteristics of two perovskites and a blend of mixed oxides prepared by reactive grinding and citrate complex method have been comparatively investigated using several techniques (X-ray, BET,  $\text{H}_2$ -TPR, chemisorption,  $\text{O}_2$ -TPD). XRD results confirm the successful substitution of Co by Cu in the lattice of  $\text{La}(\text{Co,Cu})\text{O}_3$  perovskite. The ground materials with smaller particle sizes and larger surface area show more thermal stability than does the citrate-derived sample under the same reducing conditions. Due to a lower surface area and nonporous structure, the conventional sample adsorbed a smaller amount of oxygen on the surface sites and on the vacancies compared with the other catalysts.*

### I - INTRODUCTION

Perovskites have been of interest in applied fields of both physics and chemistry because of their attractive characteristics including the electric, magnetic, and optical properties. Transition metal-containing perovskite-type oxides have shown potential catalytic applications in both oxidation and reduction reactions [1].  $\text{LaCoO}_3$ , for example, is one of the typical mixed oxides of this family having a rhombohedral distortion of the cubic perovskite structure which has been an excellent candidate for three-way-catalyst for three decades [1]. Moreover, cobaltate perovskite-type oxides were thoroughly investigated and exploited as catalysts or catalyst precursor for the oxidation of CO and hydrocarbons, NO<sub>x</sub> decomposition, hydrogenation and hydrogenolysis [2-4]. The deformation or introduction of another transition metal into the perovskite lattice both lead to a significant change in the electronic and

chemical properties. The characteristics of such materials are, however, strongly dependant on the preparative routes. The present work reports the comparative characteristics of two  $\text{LaCo}_{0.7}\text{Cu}_{0.3}\text{O}_3$  perovskites synthesized by different recipes and also examines the reduction oxidation of such materials in order to provide a novel way achieving a homogeneously dispersed Co-Cu metal for several catalytic applications [4 - 7].

### II - EXPERIMENTAL

$\text{La}(\text{Co,Cu})\text{O}_3$  perovskite-type mixed oxides synthesized by mechano-synthesis and by citrated complex method were reported in detail in Refs. [5-7]. In this present study, a reference sample,  $\text{LaCoO}_3 + 5.0 \text{ wt\% Cu}_2\text{O}$ , was prepared by grinding a mixture of the ground perovskite  $\text{LaCoO}_3$  having a specific surface area of 43  $\text{m}^2/\text{g}$  with  $\text{Cu}_2\text{O}$  oxide (10:1 molar ratio) at ambient temperature.

The chemical analysis (Fe, Co, Cu) of the perovskites was performed by atomic absorption spectroscopy using a Perkin-Elmer 1100B spectrometer. The specific surface area of all obtained samples was determined by nitrogen adsorption equilibrium at  $-196^{\circ}\text{C}$  using an automated gas sorption system (NOVA 2000; Quantachrome). The perovskite phase was examined by powder X-ray diffraction (XRD) using a SIEMENS D5000 diffractometer with  $\text{CuK}\alpha$  radiation ( $\lambda = 1.54059 \text{ nm}$ ). Temperature programmed characterization was carried out using a flow system (RXM-100, Advanced Scientific Designs, Inc.). Prior to each TPR analysis, a 40-80 mg sample was calcined at  $500^{\circ}\text{C}$  for 90 min under flowing 20%  $\text{O}_2/\text{He}$  (20 ml/min, ramp  $5^{\circ}\text{C}/\text{min}$ ). Then, the sample was cooled to room temperature under flowing pure He (20 mL/min).  $\text{H}_2$ -TPR of the catalysts was then carried out by ramping under 5vol% of  $\text{H}_2/\text{Ar}$  (20 ml/min) from room temperature up to  $800^{\circ}\text{C}$  ( $5^{\circ}\text{C}/\text{min}$ ). The hydrogen consumption was determined using a TCD with a reference gas of same composition as the reducing gas ( $\text{H}_2/\text{Ar}$ ). For each  $\text{O}_2$ -TPD test, the reduced sample was performed by ramping under 20 mL/min He (5 vol.%) from room temperature to  $900^{\circ}\text{C}$  ( $5^{\circ}\text{C}/\text{min}$ ). The effluent gas was passed through a cold trap (dry ice/ethanol) in order to remove water prior to detection (TCD, MS).

Chemisorption of  $\text{H}_2$  at  $100^{\circ}\text{C}$  was carried out after running  $\text{H}_2$ -TPR experiment. The first isotherm (total adsorption) is consisted both physisorbed and chemisorbed gas. The second adsorption isotherm is described as physisorption. The difference between the first and the second isotherm yields a chemisorption

curve. The total volume of chemisorbed gas was determined by extrapolating the straight-line portion between the adsorption isotherms to zero pressure.

### III - RESULTS AND DISCUSSION

#### 1. X-Ray diffraction

Figure 1 shows comparative XRD patterns of two Cu-Cu perovskite samples prepared by different recipes. All samples show the well-crystallized perovskite structure with the typical reflections at  $23.3$ ,  $33.0$ ,  $40.6$ ,  $47.3$ ,  $53.6$  and  $58.7^{\circ}$ . For  $\text{Cu}_2\text{O-LaCoO}_3$  sample prepared only by mechanical mixing of  $\text{Cu}_2\text{O}$  with  $\text{LaCoO}_3$ , beside of the presence of perovskite phase, there appearances some peaks at  $36.8$  and  $38.8^{\circ}$  characterizing to the  $\text{Cu}_2\text{O}$  and  $\text{CuO}$  respectively (Fig. 1). The absence of these peaks in the XRD patterns of both the ground ( $\text{LaCo}_{0.7}\text{Cu}_{0.3}\text{O}_3\text{-M}$ ) and the conventionally citrated ( $\text{LaCo}_{0.7}\text{Cu}_{0.3}\text{O}_3\text{-C}$ ) sample indicates that almost copper ions locate in the perovskite lattice. The diffraction angle at  $2\theta \approx 32.8\text{-}33.0$  observed in XRD spectrum of the ground  $\text{LaCo}_{0.7}\text{Cu}_{0.3}\text{O}_3$  (-M) modestly shifts to the lower value compared with that of the copper free-cobaltate-perovskite ( $\text{Cu}_2\text{O}/\text{LaCoO}_3$ ). Thus, the introduction of copper ions into the cobaltate lattice leads to a slightly distorted perovskite structure [6]. Figure 1 also shows that a diffraction peak width of ground samples is always rather broader than that of the traditional perovskite. This indicates that the particle size of the formers is smaller than the-one of the latter as estimated using the Scherrer equation and presented in table 1 [8, 9].

Table 1: Physical properties of samples

Samples	Recipe	$T_{\text{cal}}$ ( $^{\circ}\text{C}$ ) <sup>1</sup>	$S_{\text{BET}}$ ( $\text{m}^2/\text{g}$ )	D ( $\text{nm}$ ) <sup>2</sup>	$V_{\text{H}_2}$ ( $\text{ml}/\text{g}$ ) <sup>3</sup>	Composition (wt.%)			
						$\text{Na}^+$	Co	Cu	$\text{Fe}^4$
$\text{LaCo}_{0.7}\text{Cu}_{0.3}\text{O}_3\text{-C}$	Citrate	800	4.7	$> 35$	0.48	-	16.68	6.03	-
$\text{LaCo}_{0.7}\text{Cu}_{0.3}\text{O}_3\text{-M}$	Mechano	250	37.0	10.8	0.66	0.05	16.15	5.65	0.64
$\text{Cu}_2\text{O}/\text{LaCoO}_3$	Mechano	120	16.8	10.9	0.62	0.39	20.04	3.28	4.78

1 Calcination temperature.

2 D: crystal domain estimated from the Scherrer equation from X-ray line broadening

3  $\text{H}_2$ -chemisorbed uptake at  $100^{\circ}\text{C}$ .

4 Iron impurity from mechano-synthesis [5].

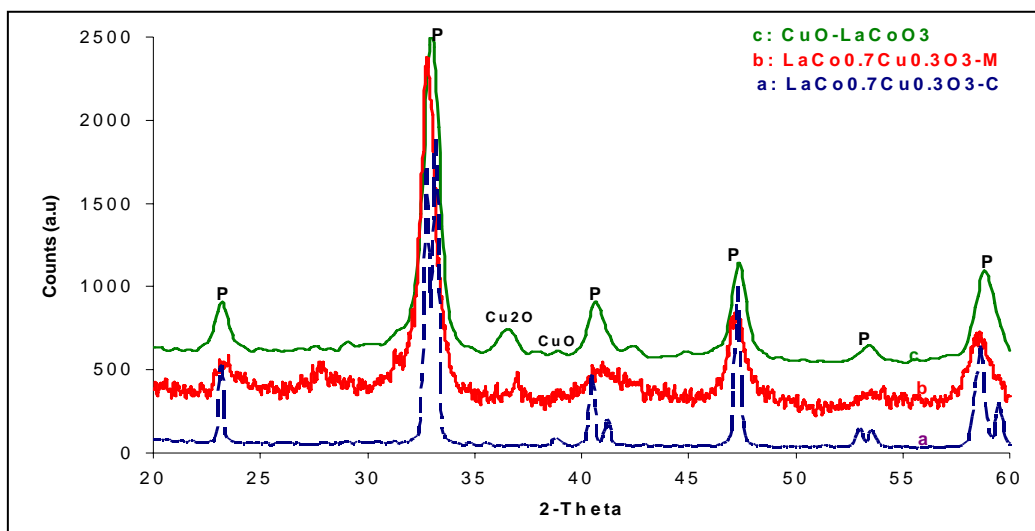


Figure 1: XRD patterns of samples

## 2. Composition and surface area

The composition and some typical physical characteristics for three samples are collected in Table 1. The specific surface area of the conventional perovskite ( $\text{LaCo}_{0.7}\text{Cu}_{0.3}\text{O}_3\text{-C}$ ) is much lower than that of the two ground samples, in agreement with several results previously reported [2-3, 5-7]. This demonstrates that BET surface area of the two powered samples is strongly dependant on the preparation methods. Furthermore, the pore size determination of catalysts was taken into account to consider the effects of the preparative routes to their external surface and their porous texture. Figure 2 presents the BJH pore size

distribution for both the ground and conventional  $\text{LaCo}_{0.7}\text{Cu}_{0.3}\text{O}_3$  perovskite. As thoroughly discussed in several previous contributions [3, 5 - 7], the ground perovskites are prepared at a relatively low temperature ( $\sim 40^\circ\text{C}$ ) and their synthesis conditions can be easily controlled. Moreover, the addition of additives during the grinding step results in an increased specific surface area, separated nanocrystal domains and a decreased volume of the grain boundaries [9, 10]. Simultaneously, the ultrafine perovskite particles (10-20nm) are usually spherical, uniformly size, which is confirmed by microscopy techniques in our previous publications [6, 9].

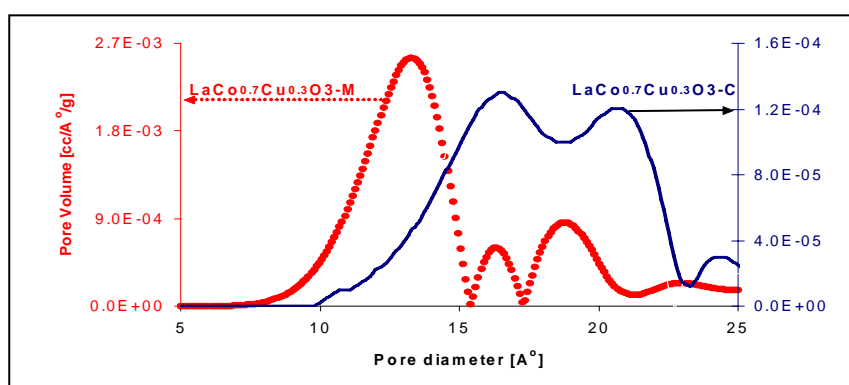


Figure 2: BJH pore size distribution for the ground (-M) and conventional (-C)  $\text{LaCo}_{0.7}\text{Cu}_{0.3}\text{O}_3$  perovskites

There are therefore many slit-shaped spaces between nanoparticles or micropores with diameters of 12 Å. The ground perovskites contain not only the smaller intra-particle pores but also larger pores consisting of the voids between pelletal particles (Fig. 2). In contrast, the conventional perovskite  $\text{LaCo}_{0.7}\text{Cu}_{0.3}\text{O}_3(-\text{C})$

shows larger pore sizes and lower pore volume, compared with the ground sample (Fig. 2). In the latter case, the pore volume is assumed from the void regions between larger rough particles. The external surface area is therefore rather low (table 1).

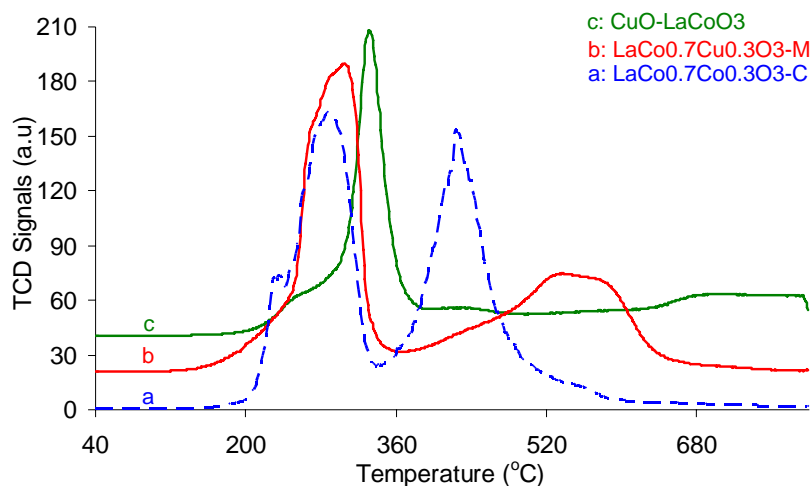


Figure 3:  $\text{H}_2$ -TPR profiles of samples

### 3. Reducibility

In order to investigate the reducibility of all samples,  $\text{H}_2$ -TPR experiments have been carried out from room temperature to 800°C. The  $\text{H}_2$ -TPR curves reported in figure 3 show two main peaks for all samples, implying the occurrence of a multiple-step reduction. According to the literature and the calculation of  $\text{H}_2$ -blance, the lower temperature peak, likely composed of two peaks with maxima around 300°C, is ascribed to the simultaneous reduction of both  $\text{Co}^{3+}$  and  $\text{Cu}^{2+}$  in the perovskite lattice to  $\text{Co}^{2+}$  and  $\text{Cu}^0$  for the two perovskite samples [6, 7, 9]. The reduction of  $\text{Co}^{2+}$  to  $\text{Co}^0$  requires a higher temperature and therefore the other peak is attributed to the formation of metallic cobalt. However, there is a small difference in a higher reduction temperature between the ground and conventional perovskite. The second peak of the ground sample (-M) is slightly higher than that of the conventional perovskite  $\text{LaCo}_{0.7}\text{Cu}_{0.3}\text{O}_3(-\text{C})$ . While the citrate-derived sample shows a

sharp peak with a maximum at 440°C, the ground perovskite gives a broad peak from 380 to 640°C because of the reduction of several distinct  $\text{Co}^{3+}$  environments in the crystallite structure in a wide temperature range. Indeed, the ground perovskites prepared by mechano-synthesis always produce a plentiful system of grain boundary and cobalt ions. Thus, cobalt and copper ions on the edge of the crystal dislocations are more reducible than those in the bulk [6, 10]. A comparison in area between the lower and higher peak points out that the ratio of the first and the second peak area is close to 1 for the conventional perovskite, but much higher than 1 for the ground sample. This suggests only the formation of  $\text{Cu}^0$  and  $\text{Co}^{2+}$  at the end of the first peak for the citrate-derived sample. In contrast, the first peak area calculated is much larger than the second one in the case of  $\text{LaCo}_{0.7}\text{Cu}_{0.3}\text{O}_3(-\text{M})$ , demonstrating the formation of a small amount of  $\text{Co}^0$  in addition to the presence of  $\text{Co}^{2+}$  and  $\text{Cu}^0$  at the first reduction

step [10].

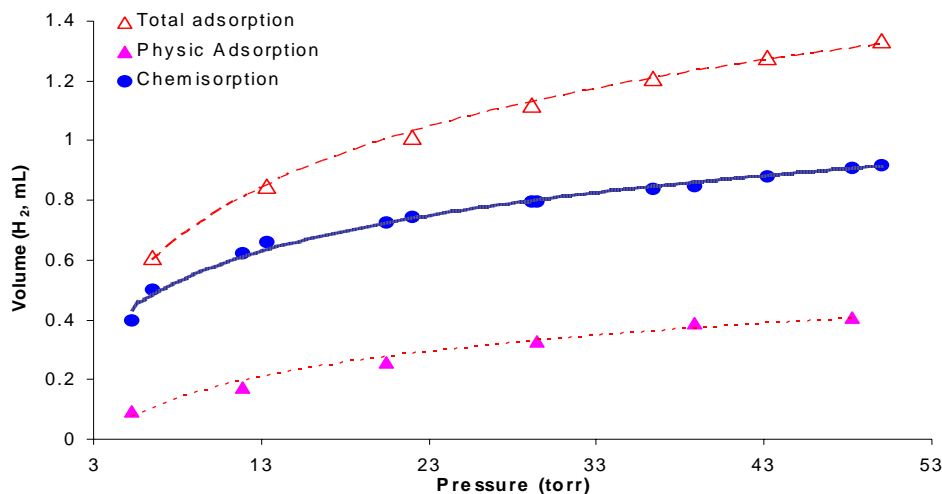


Figure 4: Chemisorption of the ground  $\text{LaCo}_{0.7}\text{Cu}_{0.3}\text{O}_3\text{-M}$  at  $100^\circ\text{C}$

It is very interesting to observe that  $\text{H}_2$ -TPR shaped-profile of the mixed  $\text{Cu}_2\text{O}/\text{LaCoO}_3$  sample is much different from those of the two perovskites. Firstly, the first reduction step takes place at a higher temperature, indicating that the reduction of extra-lattice copper is more difficult than intra-lattice copper. In addition, the second peak displays a very long tail in the higher temperature of reduction.

The quantitative reducible percentage of each metal (Co, Cu) from the  $\text{H}_2$ -TPR results is known to be a difficult task because of a simultaneous reduction of both  $\text{Co}^{3+}/\text{Co}^{2+}$ ,  $\text{Cu}^{2+}/\text{Cu}^0$  and a small amount of  $\text{Co}^{2+}/\text{Co}^0$  at lower temperatures. Instead of being determined the metal dispersion, hydrogen chemisorption has been performed at  $100^\circ\text{C}$  to compare the reduced metal areas between the studied samples. Figure 4 depicts representative  $\text{H}_2$ -adsorption curves of the ground  $\text{LaCo}_{0.7}\text{Cu}_{0.3}\text{O}_3\text{-M}$  pre-reduced at  $500^\circ\text{C}$  under hydrogen atmosphere for 90 min. Chemisorption data of the reduced forms expressed as the adsorbed hydrogen volume per unit mass of the catalyst are presented in table 1. The  $\text{H}_2$ -chemisorbed uptake corresponding to the metal surface area is proportional to the dispersion of the reduced samples. It is noted that, the cobalt sites can

strongly adsorb hydrogen at  $100^\circ\text{C}$  while copper does not [11]. Therefore, there is no significant difference in  $\text{H}_2$ -uptake between the blend of oxides and the ground sample (Table 1). Compared with the two ground samples, a remarkably lower  $\text{H}_2$ -chemisorbed volume of the conventional perovskite (-C) may be due to the low dispersion. Indeed, the reduction of citrate-derived perovskite at a lower temperature leads to the easy sintering of the reduced metal phase at a pretreatment temperature for a periodic time. This results in a substantially decreased metal surface area and consequently a dramatically declined dispersion.

#### 4. Temperature $\square$ programmed desorption of oxygen

$\text{O}_2$ -TPD chromatograms ( $m/z = 32$ ) of all samples displayed in figure 5 show two main peaks, the former with the maximum in the wide temperature range of  $300 - 670^\circ\text{C}$  and the latter with the maximum in the range of  $680 - 840^\circ\text{C}$ . The amount of oxygen corresponding to the low-temperature-peak is very small for all catalysts. The first peak, usually referred to as an  $\alpha$  peak, is attributed to oxygen species weakly bound to the surface of perovskites [5, 6, 10]. The intensity of this peak is proportional to

the specific surface area because the  $\alpha$ -oxygen released at a lower temperature is proposed to be adsorbed on the specific sites of the perovskite surface [6, 10]. Therefore, a small amount of  $\alpha$ -oxygen observed in Fig. 5 for the conventional perovskite is understandable. The higher temperature signal, designed as the  $\beta$  peak, is assigned to the reduction of  $\text{Co}^{3+}$ ,  $\text{Cu}^{2+}$  to lower oxidation states in the  $\text{La}(\text{Co,Cu})\text{O}_3$

structure and the generation of oxygen vacancies [10]. Thus, it is not surprising to observe no clear correlation between the amount of  $\beta$ -oxygen adsorbed and the specific surface area (table 1 and Fig. 5). The  $\beta$ -oxygen desorption sites are supposed to be surface anionic vacancies ( $\square$ ) from desorption of the surface lattice oxygen [5] as described in reaction below:

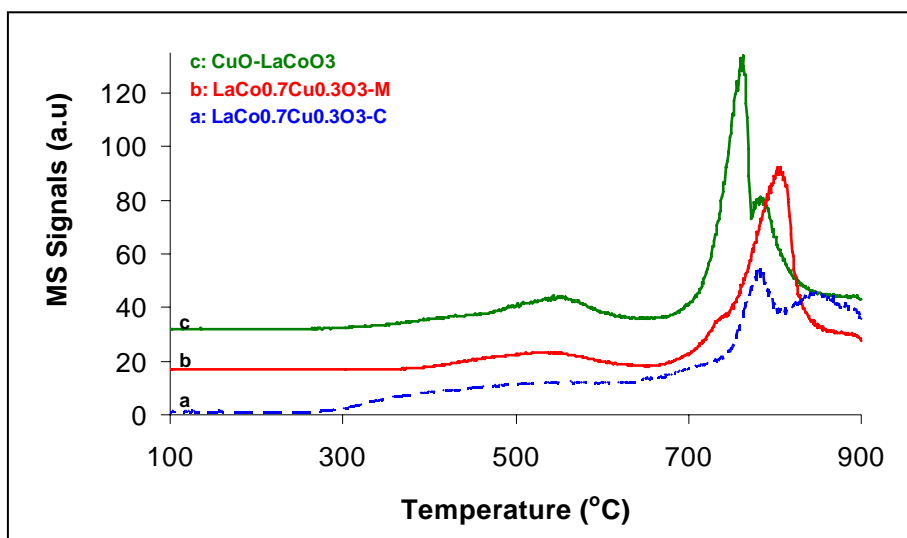
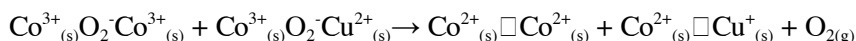


Figure 5:  $\text{O}_2$ -TPD spectra of samples

Furthermore, surface lattice oxygen is generated by the diffusion of the oxygen from the bulk to the surface [6, 10, 12]. The concentration of  $\text{Co}^{2+}$  pairs and dual  $\text{Co}^{2+}$ - $\text{Cu}^+$  sites is believed to be higher on the edge and/or in the grain boundaries than on the bulk. This explains the lower amount of  $\beta$ -oxygen desorbed on the conventional perovskite which has very low external surface area.

#### IV - CONCLUSIONS

The characteristics and the reducibility of two Co-Cu based perovskites and a mixed  $\text{Cu}_2\text{O}/\text{LaCoO}_3$  reference sample prepared by different preparative recipes have been investigated. X-ray diffraction results indicate the presence of both copper and cobalt sites in

the perovskite framework. The ground samples have smaller crystal domains and thus higher specific surface area. They usually consist of a cluster of elementary nanoparticles which lead to the formation of micro-pores while the conventional sample is almost nonporous structure. The texture of catalysts has strongly affected the reducibility of the transition metals and oxygen mobility in the perovskite lattice. The citrate-derived sample is less thermal stability than the ground perovskite under reducing atmosphere. The ground material comprises numerous distinct  $\text{Co}^{3+}$  cations in perovskite lattice that are reduced at different temperatures. In both cases, the complete reduction of  $\text{Co}^{3+}$  to  $\text{Co}^0$  occurs in two steps whereas copper is directly reduced from  $\text{Cu}^{2+}$  to  $\text{Cu}^0$ . The presence of both copper in the

perovskite lattice has a strong promotion in the reduction of  $\text{Co}^{3+}/\text{Co}^{2+}$  and  $\text{Co}^{2+}/\text{Co}^0$  by decreasing reduction temperature, whereas the appearance of extra-lattice copper has an insignificant effect on the reducibility of cobalt sites. These results may lead to develop a new way to produce highly dispersed Co-Cu metals based on the  $\text{La}(\text{Co,Cu})\text{O}_3$  perovskite precursors.

The amount of both  $\alpha$ - and  $\beta$ -oxygen adsorption released from ground materials ( $\text{Cu}_2\text{O}/\text{LaCoO}_3$  and  $\text{LaCo}_{0.7}\text{Cu}_{0.3}\text{O}_3\text{-M}$ ) is always higher than that from the conventional perovskite ( $\text{LaCo}_{0.7}\text{Cu}_{0.3}\text{O}_3\text{-C}$ ). It should be correlated with the specific surface area and the location and coordination number of cobalt sites in the ground perovskite structure.

#### REFERENCES

1. M. A. Pena and J. L. G. Fierro. *Chem. Rev.*, 101, 1981 - 2017 (2001).
2. V. Szabo, M. Bassir, J. E. Gallot, A. V. Neste, S. Kaliaguine. *Appl. Catal. B* 42, 265 - 277 (2003).
3. R. Zhang, H. Alamdari, S. Kaliaguine. *J. Catal.*, 242, 241 - 253 (2006).
4. J. O. Petunchi, J. L. Nicastro, and E. A. Lombardo. *J. C. S. Chem. Com.*, 467 - 468 (1980).
5. S. Kaliaguine, A. V. Neste, V. Szabo, J. E. Gallot, M. Bassir, R. Muzychuk. *Appl. Catal. A* 209, 345 - 358 (2001).
6. N. Tien-Thao, H. Alamdari, M. H. Zahedi-Niaki, S. Kaliaguine. *Appl. Catal., A* 311, 204 - 212 (2006).
7. N. Tien-Thao, M. H. Zahedi-Niaki, H. Alamdari, S. Kaliaguine. *J. Catal.* 245, 348 - 357 (2007).
8. H. P. Klug, L.E. Alexander. *Procedures for Polycrystalline and Amorphous Materials*, John Wiley & Sons, New York/London, 1962.
9. N. Tien-Thao, M. H. Zahedi-Niaki, H. Alamdari, S. Kaliaguine. *Appl. Catal. A*, 326, 152 - 163 (2007).
10. S. Royer, A.V. Neste, R. Davidson, S. McIntyre, and S. Kaliaguine. *Ind. Eng. Chem. Res.*, 43, 5670 - 5680 (2004).
11. N. Tien-Thao, M. H. Zahedi-Niaki, H. Alamdari, S. Kaliaguine. *Int. J. Chem. React. Eng.* Vol. 5, A82 (2007).
12. L. Lisis, G. Bagnasco, P. Ciambelli, S.D. Rossi, P. Porta, G. Russo, and M. Turco. *J. Solid State Chem.*, 146, 176 - 183 (1999).

*Corresponding author:* **Nguyen Tien Thao**

Faculty of Chemistry,  
College of Sciences, Vietnam National University, Hanoi.